Available online at www.sciencedirect.com
ScienceDirect
Trans. Nonferrous Met. Soc. China 24(2014) 2232−2238
Transactions of Nonferrous Metals Society of China
www.tnmsc.cn

Effects of process parameters on mechanical properties and microstructures of creep aged 2124 aluminum alloy

Li-hua ZHAN[1,2], Yan-guang LI[1,2], Ming-hui HUANG[1,2]

1. State Key Laboratory of High-performance Complex Manufacturing, Central South University, Changsha 410083, China;
2. School of Mechanical and Electrical Engineering, Central South University, Changsha 410083, China

Received 17 October 2013; accepted 21 April 2014

Abstract: A series of tests were carried out to investigate the effects of process parameters on mechanical properties and microstructures of 2124 aluminum alloy in creep aging process. The results show that creep strain and creep rate increase with the increase of aging time, temperature and applied stress. The hardness of specimen varies with aging time and stress in a low-to-peak-to-low manner. No significant effect of temperature on hardness of material is seen in the range of 185−195 °C. The optimum mechanical properties are obtained at the conditions of (200 MPa, 185 °C, 8 h) as the result of the coexistence of strengthening S'' and S' phases in the matrix by transmission electron microscopy (TEM). TEM observation shows that applied stress promotes the formation and growth of precipitates and no obvious stress orientation effect is observed in the matrix.
Key words: aluminum alloy; creep aging behavior; age hardening; mechanical property; microstructure; process parameter

1 Introduction

In aerospace industry, increasing large integral structures with complex curvature and high ribs are required in order to reduce the weight and manufacturing cost [1]. For these reasons, creep age forming (CAF), also called aging forming, is explored and has been used to fabricate large-scale integral parts in military and civil airplanes [2,3]. This forming method is a process consisting of mechanical formation and aging treatment of part, which takes place in the autoclave [4]. In CAF process, once the part to be formed attaches the tool configuration, it is then held by pressure or mechanical load for a certain time at a selected temperature. During this period, the elastic strain is in part converted to plastic strain due to stress relaxation and the constituents of metal precipitate, improving mechanical strengths. Different from other conventional forming techniques, the prominent feature of this technology is that the loading stress in the component is normally less than its yield strength and less residual stress occurs in the formed part [5]. Most importantly, shaping of part and property enhancement are accomplished simultaneously [6,7].

Extensive researches on creep aging behavior of metals and alloys (such as creep mechanism, microstructure and constitutive equation) have been carefully carried out over the past decades. LI et al [8] studied creep mechanisms of as-cast Mg−5Zn−2.5Er alloy by analysis of stress exponent and activation energy, and found that there is a transition region between grain boundary sliding (GBS) dominated creep and dislocation creep. LIN et al [9] investigated the effects of applied stress and creep aging temperature on the precipitation in 2124-T851 aluminum alloy. They found that the precipitation is very sensitive to the applied stress and creep aging temperature. SKROTZKI et al [10] claimed that a threshold value of stress has to be exceeded for the formation of preferentially-oriented, plate-shaped precipitate phases in the tensile stress aged samples of Al−Cu−Mg−Ag alloy and Al−Cu alloy. CHEN et al [11] suggested that external stress induces the precipitation of preferred orientation of precipitates θ'

Foundation item: Project (51235010) supported by the National Natural Science Foundation of China; Project (2010CB731700) supported by the National Basic Research Program of China; Project (20120162110003) supported by PhD Programs Foundation of Ministry of Education of China
Corresponding author: Li-hua ZHAN; Tel: +86-731-88830254; E-mail: yjs-cast@csu.edu.cn
DOI: 10.1016/S1003-6326(14)63338-0

and Ω in Al−Cu and Al−Cu−Mg−Ag alloys, respectively. ZHU et al [12] pointed out that the stress-orientation effect is associated with the applied stress, aging temperature and time, and copper content in creep aging of Al−Cu alloy. HUANG et al [13] built the constitutive model for 7B04 aluminum alloy from uniaxial tensile creep aging tests. HO et al [4] developed a set of unified aging-creep constitutive equations based on creep damage model to describe creep behavior for 7010 aluminum alloy.

Although many investigations were performed on creep aging, there are a few reports with regard to process parameters and their effects on mechanical properties and microstructure evolution. In this work, using 2124 aluminum alloy as model material, the effects of process parameters including aging time, aging temperature and loading stress on mechanical properties and microstructures of 2124 aluminum alloy in creep aging process are examined in detail, which can provide a basic theory for practical applications of CAF in industry.

2 Experimental

2.1 Specimen preparation

The chemical composition of the commercial 2124 aluminum alloy applied in this work is listed in Table 1. The specimens were machined from as-received sheet with 3 mm in thickness, as shown in Fig. 1. Then the specimens with gage length of 50 mm were subjected to solution heat treatment at 490 °C for 50 min followed by water quenching at room temperature.

Table 1 Chemical composition of 2124 aluminum alloy (mass fraction, %)

Cu	Mg	Mn	Fe	Zn	Ti	Cr	Ni	Al
4.67	1.46	0.63	0.18	0.04	0.06	<0.01	<0.01	Bal.

2.2 Creep aging test

Constant-stress creep aging tests were carried out for 2524 aluminum alloy using creep machine. The specimen was fitted and aligned in the middle of the furnace and then the furnace was gradually heated to the aging temperature. It took about 30 min to heat the specimen from room temperature to aim temperature. When the temperature reached the goal value, the dwell time of 15 min for furnace was needed prior to creep aging test. The extensometer was then calibrated to record the creep value of specimen and external stress was applied in the whole process. Experimental data could be obtained from computer after creep tests.

2.3 Mechanical property measurement and microstructure observation

Vickers hardness measurement was made on all creep aged samples. The hardness was measured by the average value of 5 different positions using a digital microscope dimension optical hardness tester (HXD −1000TM/LCD). Tensile tests for aged samples were carried out with DDL100 electronic universal testing machine and corresponding yield strength of sample was determined by the average value of two samples aged under the same condition. Thin foils for TEM analysis were cut in the gauge length of aged specimen and machined to a thickness of 60−80 μm. Then these samples were punched to disk slices of 3 mm in diameter and continually thinned using the MIT II twin-jet electropolisher in a solution of 70% ethanol and 30% nitric acid operated at −30 °C and 15 V. Finally, JEM2100 TEM operated at 200 kV was employed to observe the microstructures.

3 Results and discussion

3.1 Creep aging behaviors of 2524 aluminum alloy

Figure 2 shows the creep strain−time curves of 2124 aluminum alloy at different temperatures (185, 190 and 195 °C) and stress levels (200, 225 and 250 MPa). From Fig. 2 it is evident that all creep curves are separated into two phases. In the first phase, the initial creep rate is extremely high and decreases gradually with time, and the second phase is steady-state creep stage with

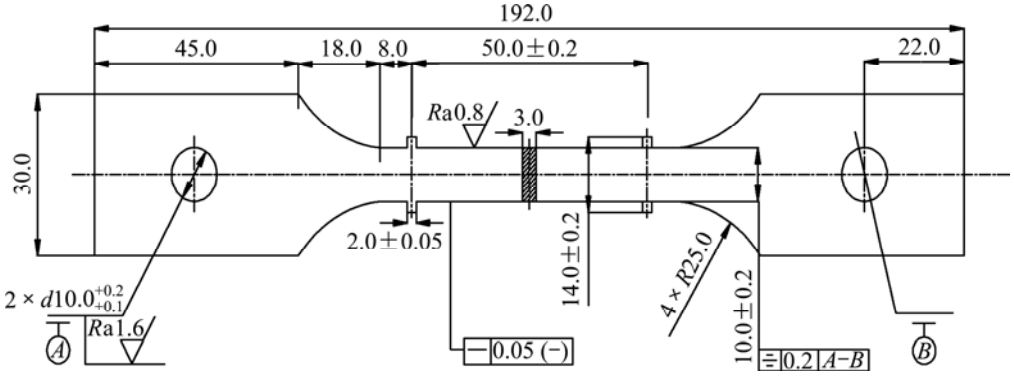

Fig. 1 Specimen geometry (unit: mm)

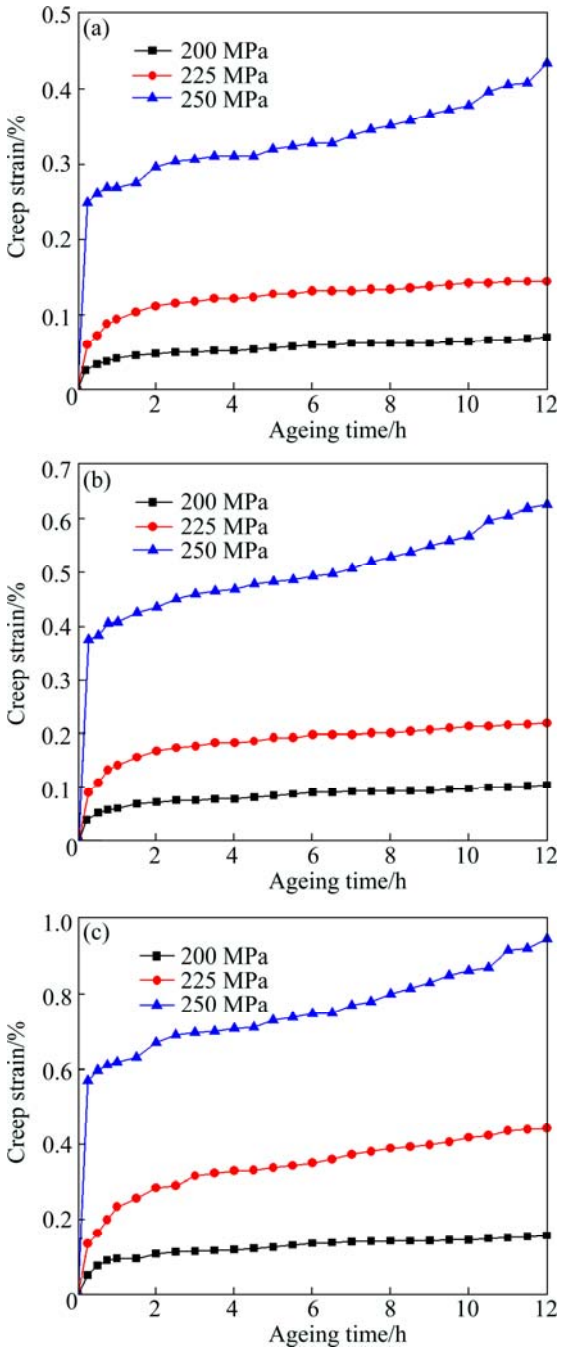

Fig. 2 Creep curves of 2124 aluminum alloy aged at different temperatures: (a) 185 °C; (b) 190 °C; (c) 195 °C

approximately constant creep rate. Usually, the creep curve contains three stages: primary creep, steady-steady creep and tertiary creep [14]. As the time required for the arrival of tertiary creep is far beyond the experimental time of 15 h, no tertiary creep was observed in this study.

The variation of creep performance with time may be due to the interaction between movements of dislocation and precipitates formed in the matrix. At the beginning of aging, the material is still in solid solution state and few precipitate phases are precipitated. In this stage, the resistance of precipitate phases to dislocation movement is slight, and hence, the creep strain and creep rate are very high. As aging time goes on, on the one hand, more and more precipitate phases are formed gradually because of thermal exposure; on the other hand, voluminous dislocations are created in α(Al) matrix phase due to the applied stress, which can provide heterogeneous nucleation sites for precipitate phase and thus promote the precipitation of precipitate phases. As the precipitate phases can pin the dislocation motions in creep aging process, the movements of dislocation are impeded, leading to a decrease in creep rate. For the secondary creep stage with characteristic of about constant creep rate, it is caused by the combined effects of working hardening and softening by dynamic recovery at high temperatures.

Comparing all curves in Fig. 2, it is found that a higher temperature leads to a higher creep strain and creep rate when keeping other testing conditions constant. Normally, creep deformation is principally controlled by dislocation sliding in grains. At temperature of 185 °C, there are many intragranular glide bands as well as a few intragranular cross-glide bands in matrix. It is generally accepted that creep is thermal-activated process that is sensitive to temperature. When temperature increases, a large number of intragranular cross-glide bands are developed, coupled with more and more dislocations forming. These make creep deform much easier. In addition, the strength of grain boundary reduces gradually as the temperature increases, resulting in grain boundary glide, which is good for material to deform [15]. It is also observed that creep strain and creep rate increase with increasing applied stress. As seen from Fig. 2, in the stress range of 200−225 MPa, the influence of stress on creep strain is not significant; however, when the stress is 250 MPa, the creep strain increases rapidly and is approximately four times that of 200 MPa. It can be reasonably inferred that creep strain is much more sensitive to high stress.

3.2 Aging hardness

An investigation was conducted on the effect of aging time on the Vickers hardness of 2124 aluminum alloy aged at different temperatures and a constant stress of 200 MPa. The experimental temperatures were 185 and 190 °C, respectively. The variation of hardness with aging time under different aging temperatures exhibits a similar trend (see Fig. 3). Noticeably, age-hardening process is strongly influenced by aging time. The hardness increased with the prolonging aging time, and came to peak value after 8 h of aging, followed by a gradual decrement. The maximum hardness for specimens aged at 185 °C and 190 °C were HV 171.5 and HV 173.5, respectively. A typical aging process, i.e.

under aging, peak aging and over aging, was observed in Fig. 3. But only a slight influence of temperature was seen on the kinetics of the age-hardening process. The hardness of sample aged at 190 °C is slightly higher than that of 185 °C creep aged one in the time range of 1−15 h.

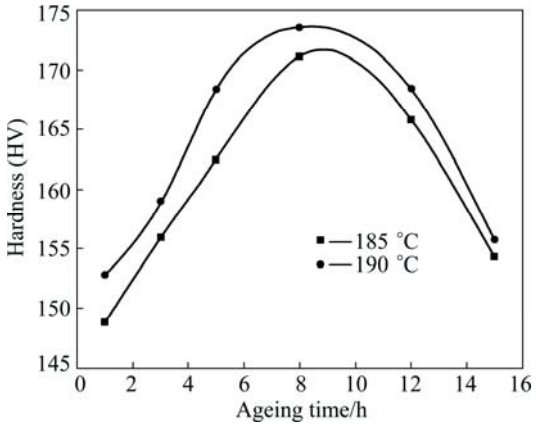

Fig. 3 Hardness curves monitored at 200 MPa and different aging temperatures

In the creep aging process, applied stress and aging temperature provide significant contributions to hardening because they both drastically promote the precipitation of precipitate phases. At the early period of aging, with the rapid formation of GP zones, the hardness increases fast. As the aging time prolongs, the GP zones are transformed into *S*″ phases and *S*′ phases. These transient phases increase the hardness of material continually up to peak value at 8 h. However, the hardness after peak aging begins to reduce with the increasing aging time because of material being in over aging stage.

The effect of loading stress on Vickers hardness of 2124 aluminum alloy samples aged at various aging temperatures for 12 h is illustrated in Fig. 4. The tensile stresses were 150, 200, 225 and 250 MPa, respectively. And the aging temperatures were 185, 190 and 195 °C.

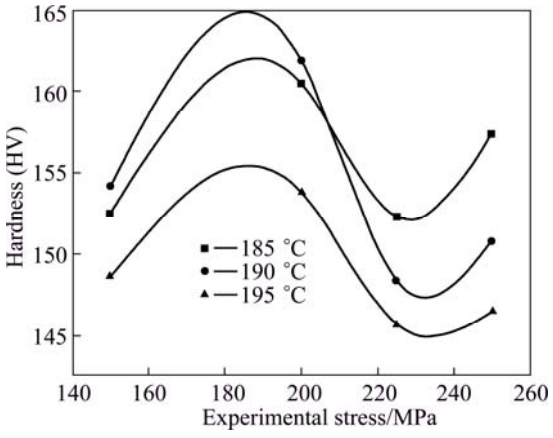

Fig. 4 Hardness curves measured at different temperatures

As seen from Fig. 4, the hardening curves present sinusoidal change with stress level whether the temperature is high or low. The minimum hardness is found at approximately 225 MPa and the maximum hardness at about 190 MPa.

3.3 Mechanical property

In light of the analysis above, it can be known that three main factors including aging time, aging temperature and loading stress affect the hardness of 2124 aluminum alloy significantly. Their influences on the yield strength of 2124 aluminum alloy were examined by means of tensile tests. The results of the effect of them on yield strength of specimens are summarized in Table 2. As seen, under stress level of 200 MPa and time ranging from 1 to 15 h, the yield strength of material increases first until it reaches peak value at 8 h, and then decreases with the increasing aging time. Moreover, under the conditions of (200 MPa, 12 h), the change in yield strength of samples with aging temperature is little, showing a tiny low-to-peak-to-low tendency. The values of yield strength at 185, 190, 195 °C correspond to 304.0, 305.5 and 298.3 MPa, respectively. However, for a higher stress level of 225 or 250 MPa, the variation trend of yield strength with the increasing temperature is different, which presents a linearly decreasing tendency (see Table 2). It can be reasonably concluded that the optimum process parameters for obtaining the best material performance are 8 h, 185 °C and 200 MPa. Among all three parameters, aging time provides the most significant contribution to the mechanical properties.

Table 2 Yield strength of 2124 aluminum alloy under different creep aging conditions

Stress/MPa	Time/h	Yield strength/MPa		
		185 °C	190 °C	195 °C
200	1	238.0	263.0	−
	3	239.5	271.9	−
	5	259.7	295.3	−
	8	329.5	322.3	−
	12	304.0	305.5	298.3
	15	280.0	290.2	−
225	12	297.6	296.8	293.8
250	12	303.4	294.3	292.7

3.4 TEM observation

In order to reveal the evolution of mechanical property with process parameters in 2124 aluminum alloy, transmission electronic microscopy (TEM) analysis of aged samples was conducted. The aging behavior of 2xxx aluminum alloy by isothermal heat

treatment has been examined in detail by several investigators [16, 17]. The generally accepted precipitation sequence is

SSSS (supersaturated solid solution)→GP zone→
S''→S'→S (Al_2CuMg)

where GP zone is transient precipitate formed by a cluster of Cu and Mg atoms; S'' and S' phases are more stable transient precipitates; S phase(Al_2CuMg) is equilibrium phase.

Figures 5(a)−(d) show the morphologies of the precipitate phases with the extension of aging time from 1 to 12 h when maintaining the loading stress of 200 MPa and aging temperature of 185 °C. For the four images, the number density and size of precipitates are significantly influenced by aging time. After aging at

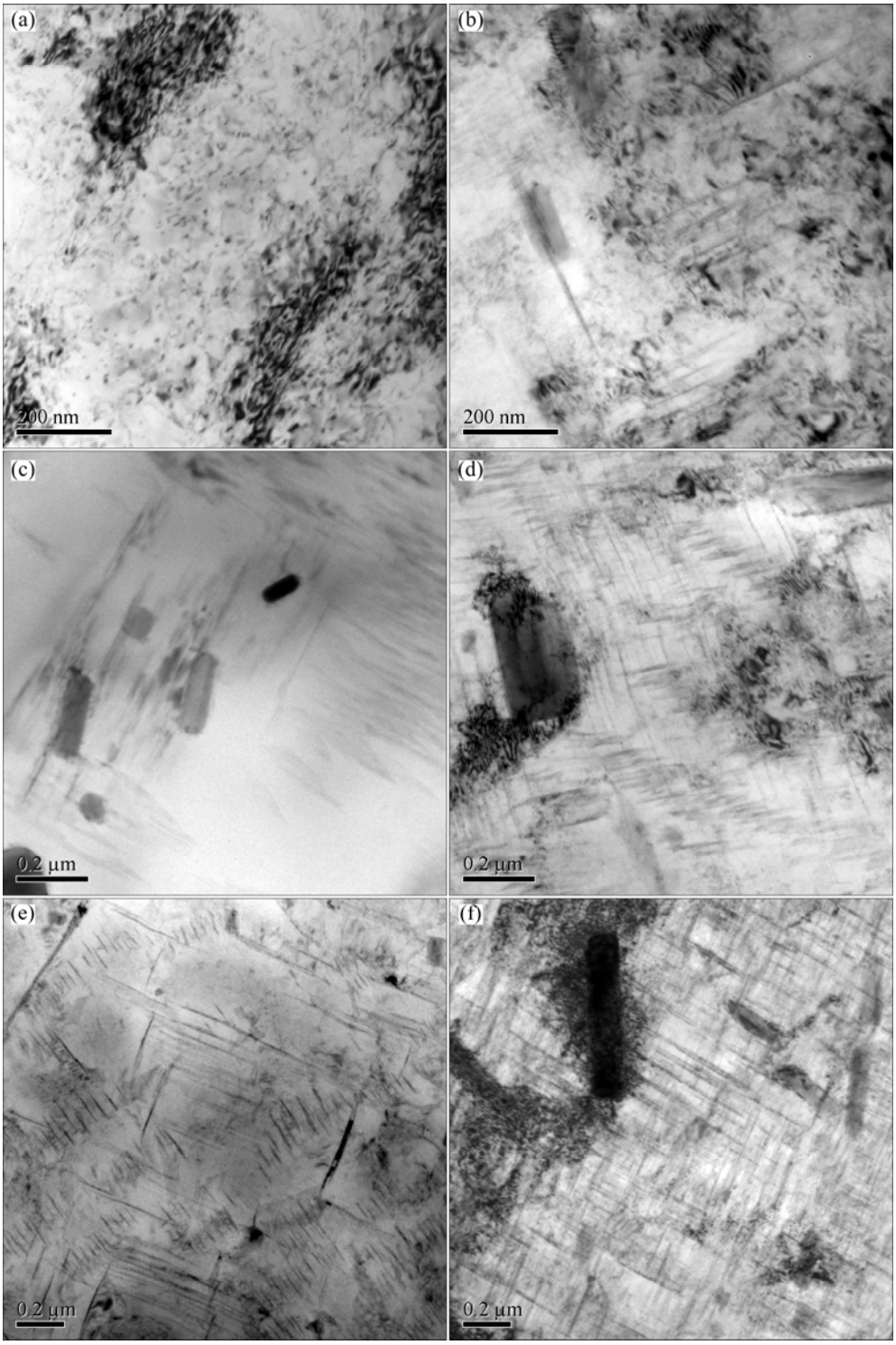

Fig. 5 TEM images of 2124 aluminum alloy creep aged under different conditions: (a) 185 °C, 200 MPa, 1 h; (b) 185 °C, 200 MPa, 3 h; (c) 185 °C, 200 MPa, 8 h; (d) 185 °C, 200 MPa, 12 h; (e) 195 °C, 200 MPa, 12 h; (f) 195 °C, 250 MPa, 12 h

185 °C for 1 h, as shown in Fig. 5(a), lots of ribbon-like or spherical *S″* phases were homogeneously precipitated from the supersaturated solid solution of 2124 aluminum alloy. The mechanical property of material increases due to the uniform distribution of *S″* phases. At 3 h (Fig. 5(b)), the quantity of spherical *S″* phases decreased while their dimensions increased, and some needle-like *S′* phases were found except for the ribbon-like or spherical *S″* phases. With time increasing to 8 h, the number of the ribbon-like or spherical *S″* phases decreased more obviously while the volume fraction of needle-like *S′* phase increased considerably, as shown in Fig. 5(c). The coexistence of the main strengthening precipitates (*S″* and *S′* phase) in Fig. 5(c) gives the best mechanical property under conditions of 200 MPa, 8 h, 185 °C. Further prolonging the aging time to 12 h (Fig. 5(d)), the ribbon-like or spherical *S″* phases almost vanished and the quantity and size of needle-like *S′* phase increased continually. However, some coarse equilibrium phases (*S* phase) are formed. This indicates that the alloy is in over aging stage and the mechanical performance drops.

The effects of aging temperature on microstructures of 2124 aluminum alloy aged at 200 MPa for 12 h are shown in Figs. 5(d) and (e). For comparison, the temperatures in Figs. 5(d) and (e) were 185 and 195 °C, respectively. Overall, it can be seen that aging temperature can accelerate the formation and growth of precipitates. From Fig. 5(d), a large number of rod-like *S′* phases (Al_2CuMg) are formed on the habit plane with typical size of 100−300 nm. Some non-coherent *S* phases are also found in Fig. 5(d). Figure 5(e) shows needle-shaped precipitate phases precipitating in different directions when aging temperature increases to 195 °C. Besides the orthogonal precipitated *S′* phase, some *S′* phases also precipitate on (111) habit plane and part of them coarsen and transform to coarse rod-like *S* phases. Due to the coarse *S* phases as well as inhomogeneous distribution of precipitates, the property of material aged under conditions of Fig. 5(e) is weaker than that of Fig. 5(d), which is directly proved by the test in Table 2.

Figures 5(e) and (f) illustrate the effect of stress on microstructures of 2124 aluminum alloy subjected to aging at 195 °C for 12 h. The stresses applied to specimen are 200 MPa in Fig. 5(e) and 250 MPa in Fig. 5(f). Compared with Fig. 5(e), it can be observed from Fig. 5(f) that higher loading stress applied during aging promotes the precipitation and growth of precipitate phases, and voluminous orthogonal *S′* phases are distributed uniformly in the Al matrix. This may be ascribed to that the applied stress of 250 MPa nearly approaches the yield strength and more dislocations are generated in the alloy, which can give numerous nucleation sites for *S′* phases [18]. No obvious stress orientation effects of precipitates are found in both Figs. 5(e) and (f). ZHU and STARKE [12] suggested that stress orientation effect is due to the misfit between precipitates and matrix.

Preferentially-oriented precipitates are nucleated in the matrix in order to cancel the misfit to reduce energy barrier, so the stress can affect the orientation of precipitates. It is known that *S′* phases prefer to nucleate heterogeneously on dislocations and grow and coarsen. Lots of dislocations can provide the requisite misfit to cancel the misfit between precipitates and matrix [18]. This accommodates the applied stress. So, there is no obvious effect of stress on the preferential alignment of *S′* phase.

4 Conclusions

1) Creep behaviors of 2124 aluminum alloy shows two stages within experimental conditions, i.e. primary and steady-state creep stages. Creep strain and creep rate increase with the increase of aging time, temperature and stress level. Creep strain is much more sensitive to high stress.

2) The hardness of 2124 aluminum alloy increases first, comes to peak value at 8 h, and then decreases with aging time.

3) Optimum mechanical performance is obtained under the conditions of 8 h, 185 °C, 200 MPa as a result of the coexistence of *S″* and *S′* phases in matrix.

4) TEM observation shows that the applied stress promotes the formation of precipitates in creep aging process and no obvious stress orientation effect is observed.

References

[1] WATCHAM K. Airbus A380 takes creep age-forming to new heights [J]. Materials World, 2004, 12(2): 10−11.

[2] ZHU A W, STARKE E A. Materials aspects of age-forming of Al−*x*Cu alloys [J]. Journal of Materials Processing Technology, 2001, 117(3): 354−358.

[3] ZHAN L H, LIN J G, DEAN T A. A review of the development of creep age forming: Experimentation, modelling and applications [J]. International Journal of Machine Tools & Manufacture, 2011, 51(1): 1−17.

[4] HO K C, LIN J, DEAN T A. Constitutive modelling of primary creep for age forming an aluminium alloy [J]. Journal of Materials Processing Technology, 2004, 153−154: 122−127.

[5] ZHAN L H, LIN J G, DEAN T A, HUANG M H. Experimental studies and constitutive modelling of the hardening of aluminium alloy 7055 under creep age forming conditions [J]. International Journal of Mechanical Sciences, 2011, 53(8): 595−605.

[6] NOVY F, JANECEK M, KRAL R. Microstructure changes in a 2618 aluminium alloy during ageing and creep [J]. Journal of Alloys and Compounds, 2009, 487(1−2): 146−151.

[7] LI Jing-feng, ZHENG Zi-qiao, LI Shi-chen, REN Wen-da, CHEN

Wen-jing. Age forming of Al alloys and ageformable Al alloys [J]. Materials Review, 2006(5): 101−103. (in Chinese)

[8] LI H, DU W B, LI J H, LI S B, WANG Z H. Creep properties and controlled creep mechanism of as-cast Mg−5Zn−2.5 Er alloy [J]. Transactions of Nonferrous Metals Society of China, 2010, 20(7): 1212−1216.

[9] LIN Y C, XIA Y C, JIANG Y Q, LI L T. Precipitation in Al−Cu−Mg alloy during creep exposure [J]. Materials Science and Engineering A, 2012, 556: 796−800.

[10] SKROTZKI B, SHIFLET G, STARKE JR E. On the effect of stress on nucleation and growth of precipitates in an Al−Cu−Mg−Ag alloy [J]. Metallurgical and Materials Transactions A, 1996, 27(11): 3431−3444.

[11] CHEN Da-qin, ZHENG Zi-qiao, LI Shi-chen, CHEN Zhi-guo, LIU Zu-yao. Effect of external stress on the growth of precipitates in Al−Cu and Al−Cu−Mg−Ag alloys [J]. Acta Metallurgica Sinica, 2004, 40(8): 799−804. (in Chinese)

[12] ZHU A W, STARKE E A. Stress aging of Al–*x*Cu alloys: Experiments [J]. Acta Materialia, 2001, 49(12): 2285−2295.

[13] HUANG Shuo, WAN Min, HUANG Lin, CHI Cai-lou, JI Xiu-sheng. Aluminum alloy creep test and its constitutive modeling [J]. Journal of Aeronautical Materials, 2008, 28(1): 93−96. (in Chinese)

[14] LIU X B, GUAN X, CHEN R S, HAN E H. Creep behavior of ageing hardened Mg−10Gd−3Y alloy [J]. Transactions of Nonferrous Metals Society of China, 2010, 20(S2): s545−s549.

[15] CHEN Yu-qiang, YI Dan-qing, PAN Su-ping, HUANG Xia, WANG Bin, ZHOU Ming-zhe. Effect of temperature on creep behavior of 2024 aluminum alloy [J]. The Chinese Journal of Nonferrous Metals, 2010, 20(4): 632−639. (in Chinese)

[16] KUMARAN S M. Evaluation of precipitation reaction in 2024 Al−Cu alloy through ultrasonic parameters [J]. Materials Science and Engineering A, 2011, 528(12): 4152−4158.

[17] BADINI C, MARINO F, VERN E. Calorimetric study on precipitation path in 2024 alloy and its SiC composite [J]. Materials Science and Engineering A, 1995, 191(1−2): 185−191.

[18] QUAN L W, ZHAO G, TIAN N, HUANG M L. Effect of stress on microstructures of creep-aged 2524 alloy [J]. Transactions of Nonferrous Metals Society of China, 2013, 23(8): 2209−2214.

工艺参数对蠕变时效 2124 铝合金力学性能和微观组织的影响

湛利华[1,2]，李炎光[1,2]，黄明辉[1,2]

1. 中南大学 国家高性能复杂制造重点实验室，长沙 410083；
2. 中南大学 机电工程学院，长沙 410083

摘 要：研究 2124 铝合金在蠕变时效过程中工艺参数对力学性能和微观组织的影响。结果表明，蠕变量和蠕变速率随着时效时间、温度、应力的增大而增大。硬度随着时间和应力的增加呈类似于先增加后减小的趋势。在实验温度 185~195 ℃ 范围内，温度对硬度的影响不大。当蠕变条件为 200 MPa、185 ℃、8 h 时，试样得到最佳的力学性能，此时试样基体内同时存在强化相 *S*″相和 *S*′相。透射电镜观察表明外加应力能促进析出相的析出和长大，基体中没有发现明显的应力位向效应。

关键词：铝合金；蠕变时效行为；时效强化；力学性能；微观组织；工艺参数

(Edited by Xiang-qun LI)